

Supporting Information

Galvanic cell reaction driven electrochemically doping of TiO₂ nanotube photoanodes for enhanced charge separation

Heng Zhu,^a Yingfei Hu,^a Kai Zhu,^b Shicheng Yan,^{*a} Lei Lu,^a Meiming Zhao,^a Hongwei Fu,^a Zhaosheng Li^a and Zhigang Zou^{a,c}

^a Eco-Materials and Renewable Energy Research Center (ERERC), Collaborative Innovation Center of Advanced Microstructures, College of Engineering and Applied Sciences, Nanjing University, No. 22, Hankou Road, Nanjing, Jiangsu, 210093, PR China. E-mail: yscfei@nju.edu.cn.

^b School of Information Science and Engineering, Nanjing University Jinling College, No. 8, Xuefu Road, Nanjing, Jiangsu 210089, P. R. China

^c National Laboratory of Solid State Microstructures, Department of Physics, Nanjing University, No. 22, Hankou Road, Nanjing, Jiangsu, 210093, PR China

Experiment Methods

Preparation of TiO₂ nanotube array electrodes. The electrochemical anodic oxidation method was used to fabricate the TiO₂ nanotube arrays film.¹ To remove the surface oxidation layer, the titanium sheet (0.2 mm thickness, 99.5% purity) was first chemically polished in the solution containing HF, HNO₃, and deionized water (1:2:7 in volume) for 30 s. The resulting titanium sheets were ultrasonically cleaned with acetone, ethanol, and deionized water, and then were anodized in 250 mL NH₄F-containing ethylene glycol (EG) solution (1g NH₄F, 245 mL EG, 5mL deionized water) at 60 V for 15 min at room temperature and the counter electrode was a platinum plate. The as-anodized samples were thoroughly cleaned with deionized water and then annealed in air at 450 °C for 2 h with a heating rate of 10 °C min⁻¹.

NaBH₄ treatment. The conductor parts of the as obtained sample where no nanotubes grown were polished with sandpaper to remove the TiO₂ compact layer on the surface of Ti sheet formed during heat treatment. The one that whole sample including nanotubes and conductor parts was immersed in 0.5 M NaBH₄ solution (W-TiO₂). The other one the conductor parts on the back and front of the photoanode were thoroughly sealed by insulating tape and only nanotubes on the sample can contact NaBH₄ electrolyte (O-TiO₂). For comparison, commercial anatase TiO₂ nano powders (0.1 g) were added to 50 mL 0.5 M NaBH₄ solution under magnetic stirring for a relative long time 3 h at room temperature.

Electrochemical doping. The TiO₂ nanotubes electrode as the working electrode were immersed in 1 M NaOH solution. Then a negative bias -1.35 V was applied in the dark at room temperature for 10 ~ 60 s.²

TiO₂ nanotube array characterizations. The morphologies of the TiO₂ nanotube photoanodes were observed by field-emission scanning electron microscope (FE-SEM; Nova NanoSEM 230, FEI). Crystal phases of these samples were determined using an X-ray

diffractometer (XRD, Rigaku Ultima III, Japan) operated at 40 kV and 40 mA using Cu K α radiation. X-ray photoelectron spectroscopy (XPS) measurements were carried out on a Thermo VG Scientific ESCALAB 250 spectrometer with monochromatized Al K α excitation. The spectral positions were corrected by normalizing the C1s spectrum at 284.6 eV, and a Shirley background was used for peak fitting. The UV-Vis absorption spectra were obtained by ultraviolet-visible spectrophotometer (UV, Shimadzu UV-2550). Electron paramagnetic resonance (EPR) was conducted with an X-band EPR spectrometer (EMX-10/12, Bruker, German) operating at a microwave frequency of 9.49 GHz at 110 K.

Electrochemical and photoelectrochemical characterization. A CHI760E electrochemical workstation (Shanghai Chenhua Company, Shanghai, China) was used to conduct the electrochemical and photoelectrochemical measurements, which were performed in a standard three-electrode cell at room temperature. The electrode except the semiconductor-electrolyte interface was thoroughly sealed with silica gel or black insulating tape. A platinum plate and saturated Ag/AgCl were used as counter and reference electrodes, respectively. All the potentials are described by referring to the Ag/AgCl reference electrode. A 500 W Xe lamp was used as the light source for photocurrent measurements. The irradiated area was circular with area of 0.28 cm² and photocurrent densities were normalized to 1 cm². Oxidation–reduction potential was measured by open circuit potential (OCP) mode. Mott-Schottky curves were measured using an electrochemical analyzer (2273, Princeton Applied Research, AMETEK, USA). The electrochemical impedance spectra (EIS) were measured using an electrochemical analyzer (Solartron 1260 + 1287, AMETEK, USA) with a 10 mV amplitude perturbation and frequencies between 100 kHz and 0.1 Hz

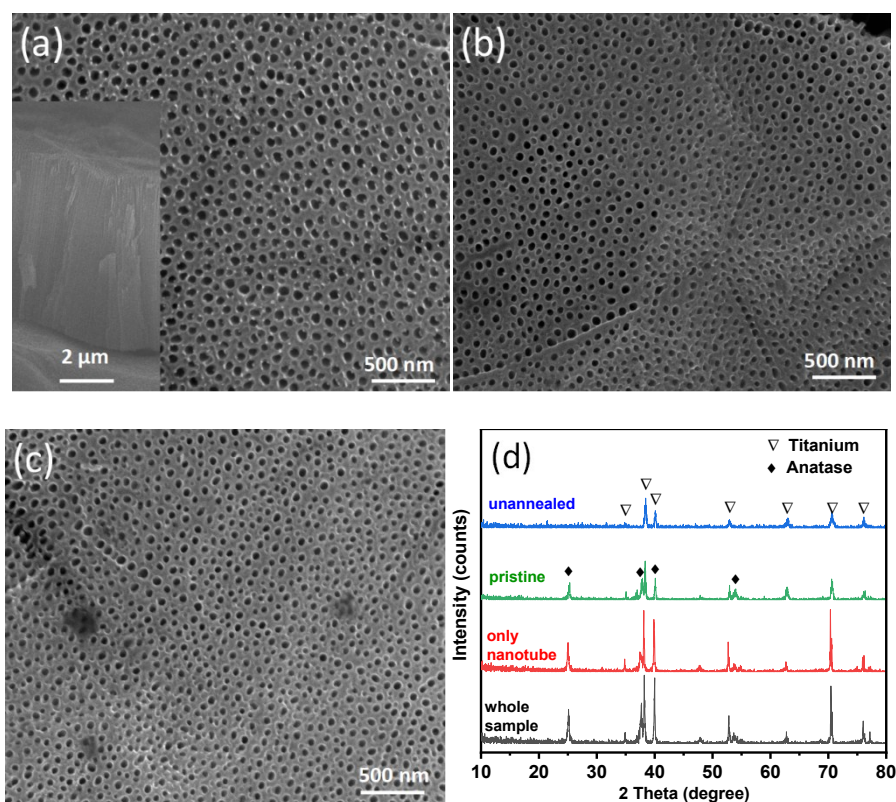


Fig. S1 SEM images of TiO₂ nanotube array electrode. (a) The as-obtained sample. The inset shows a cross-section SEM image. (b) W-TiO₂ electrode after immersing in NaBH₄ for 1 h. (c) O-TiO₂ electrode after immersing in NaBH₄ for 1 h. (d) XRD patterns. The sample after anodic oxidation (blue line) and after annealing (green line) in air at 450 °C for 2 h, the TiO₂ nanotube electrode after NaBH₄ treatment for 1 h, O-TiO₂ (red line) and W-TiO₂ (black line).

The samples obtained by anodic oxidation without annealing in air is essentially amorphous because all the diffraction peaks are assigned to Ti substrate. After heating in air at 450 °C for 2 h, the amorphous film became crystallized single-phase TiO₂ with anatase structure (JCPDS Card No. 21-1272). Morphology and structural properties of the samples were almost no varied after NaBH₄ treatment.

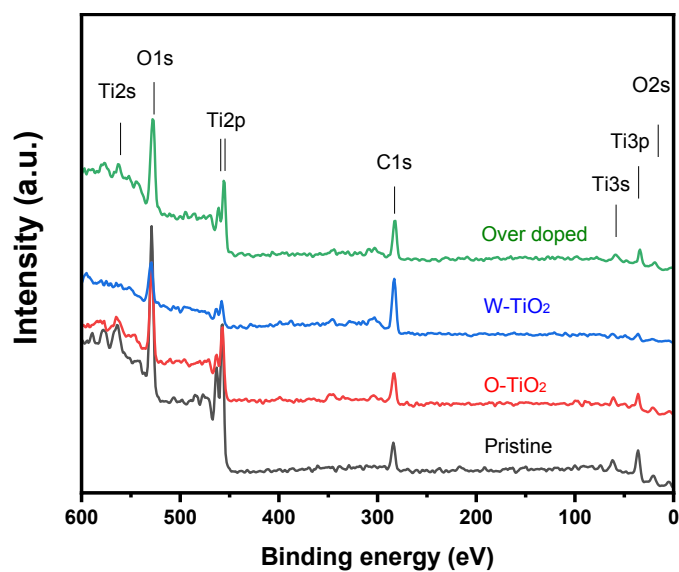


Fig. S2 Wide XPS spectrum. The pristine TiO_2 nanotube photoanodes, O-TiO_2 , W-TiO_2 and electrode electrochemical over doped in aqueous 1 M NaOH at -1.75 V 90 s.

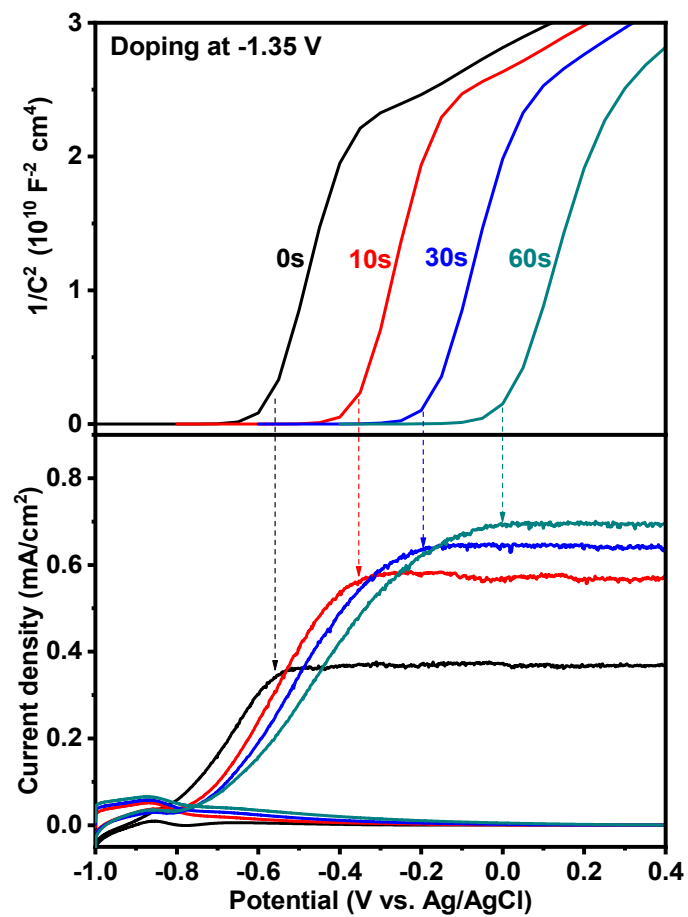


Fig. S3 The correlation of Mott-Schottky plots (top) and photocurrent density curves (bottom) of TiO_2 nanotubes electrode after electrochemical doping in 1 M NaOH solution at -1.35 V for 0, 10, 30, and 60 s. Scan rate: $20 \text{ mV s}^{-1,2}$

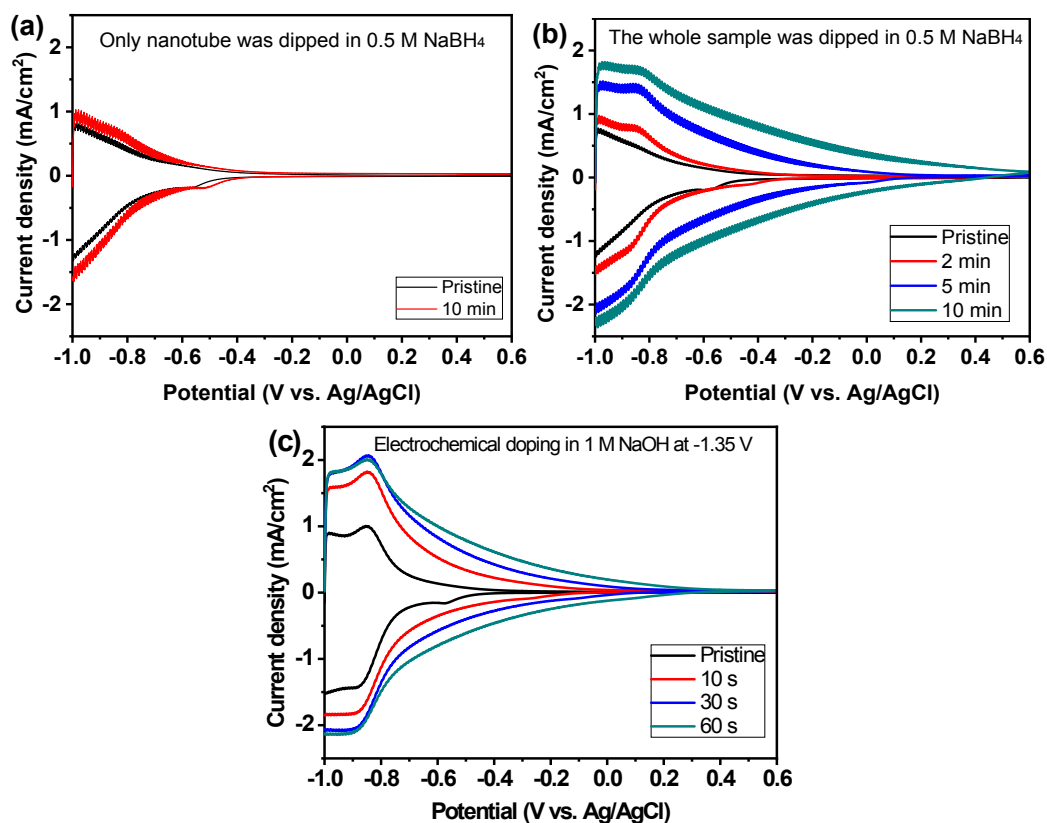


Fig. S4 (a) Cyclic voltammetry (CV) curves of the O-TiO₂ samples before and after NaBH₄ treatment for 10 min. (b) CV curves of the W-TiO₂ samples before and after NaBH₄ treatment for 2, 5, and 10 min. (c) CV curves of the samples before and after electrochemical doping in aqueous 1 M NaOH at -1.35 V for 10, 30, and 60 s. Scan rate: 500 mV s⁻¹. We can find that after NaBH₄ treatment the CV curves for W-TiO₂ are very similar with the TiO₂ nanotube array after electrochemical doping.

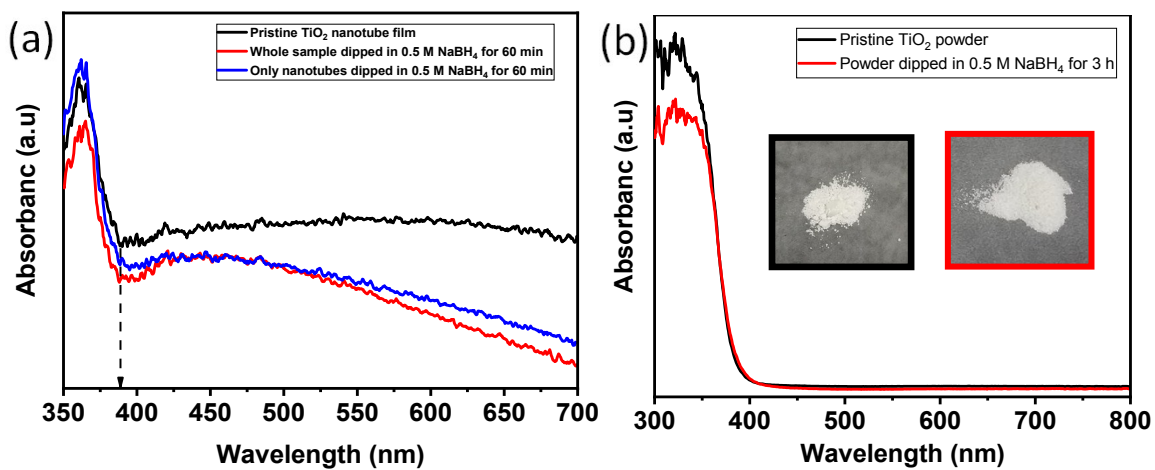


Fig. S5 (a) The UV-visible diffuse reflection spectra of TiO₂ nanotube array before and after NaBH₄ treatment for 60 min of W-TiO₂ and O-TiO₂ electrodes. (b) The UV-visible diffuse reflection spectra of TiO₂ nanoparticles before and after NaBH₄ treatment for 3 h. Inset pictures were the photo of the samples.

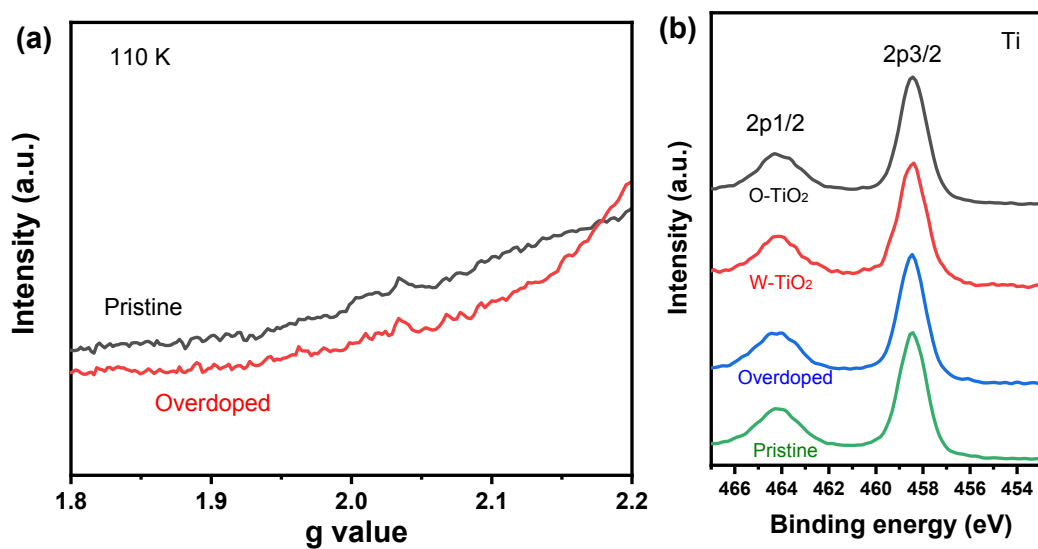


Fig. S6 (a) EPR spectra for pristine and electrochemical overdoped TiO₂ nanotube photoanodes. (b) XPS spectra of Ti2p.

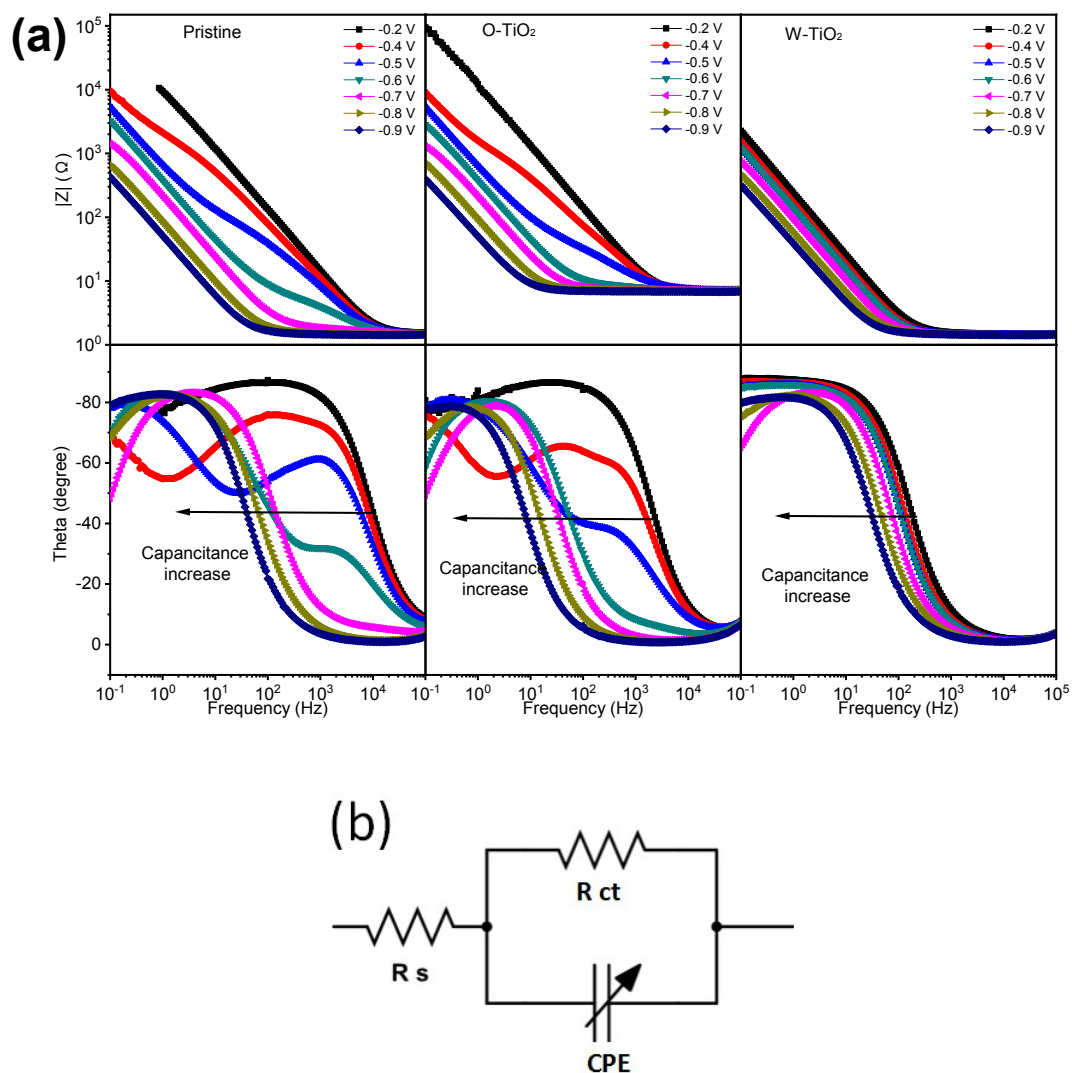


Fig. S7. Electrochemical impedance diagrams (Bode representation) of the as obtained (right), O-TiO₂ (mid) and W-TiO₂ (left) nanotube electrodes measured in 1 M NaOH in the dark. The active area of the samples was 0.28 cm² (b) Equivalent circuits used to simulate the EIS data. R_s : resistance from electrolyte and semiconductor- substrate electrical connection; R_{ct} : interfacial charge transfer resistance between semiconductor and electrolyte; CPE: capacitance for space charge layer or surface states of TiO₂ nanotube electrode.

For the pristine and O-TiO₂ when at the potential positive to -0.5 V vs. Ag/AgCl the capacitance decreases dramatically. Because at this potential charges in the surface states and nanotube walls were fully depleted which could not respond to the electrical signal. In addition, for W-TiO₂ nanotube electrodes charges in surface states and nanotube walls were not depleted

at the potential window we used because the high surface states density formed by electrochemical doping induced by the galvanic cell reaction during NaBH₄ treatment. The result is consistent with the M-S and CV results. So, we believe abundant surface states formed on W-TiO₂ *via* an electrochemical doping reaction induce by a galvanic cell reaction during NaBH₄ treatment.

Fitting parameters of EIS data obtained by using the equivalent circuit proposed in **Fig. S7**

Samples	Potential (V vs. Ag/AgCl)	CPE		R _{ct,bulk} (KΩ)	R _s (Ω)
		Q (μΩ ⁻¹ s ⁿ)	n		
Pristine TiO ₂ nanotubes	-0.9	3469	0.95	3.5	1.4
	-0.8	2083	0.94	2.3	1.5
	-0.7	825.9	0.95	2.3	1.7
	-0.3	38.0	0.88	46.8	1.4
	-0.2	16.0	0.96	48.4	1.5
O-TiO ₂	-0.9	3714	0.93	3.6	6.8
	-0.8	1916	0.94	2.3	7.1
	-0.7	494.9	0.92	7.6	7.7
	-0.3	27.3	0.89	29.6	6.6
	-0.2	13.6	0.97	74.2	7.0
W-TiO ₂	-0.9	4684	0.94	3.5	1.4
	-0.8	3062	0.94	2.6	1.4
	-0.7	1842	0.96	1.9	1.4
	-0.6	1484	0.96	7.7	1.5
	-0.5	1131	0.99	10.8	1.5
	-0.4	934.3	0.99	21.1	1.5
	-0.3	770.1	0.99	31.9	1.5
	-0.2	657.9	0.99	57.4	1.5

*The active area of the samples was 0.28 cm²

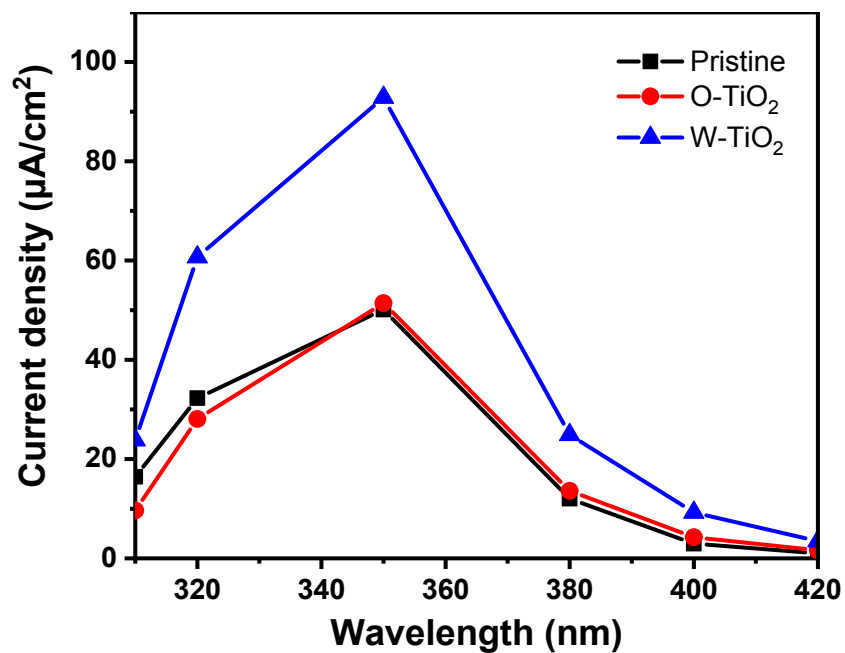


Fig. S8 Under different monochromatic light irradiation, the photocurrents for pristine TiO₂ nanotube photoanodes, O-TiO₂ and W-TiO₂ photoanodes after 10 min NaBH₄ treatment. The increased current density was not come from the visible light contribution. After NaBH₄ treatment, the charge separation efficiency for W-TiO₂ photoanodes at the ultraviolet region increased dramatically comparing to O-TiO₂ photoanodes.

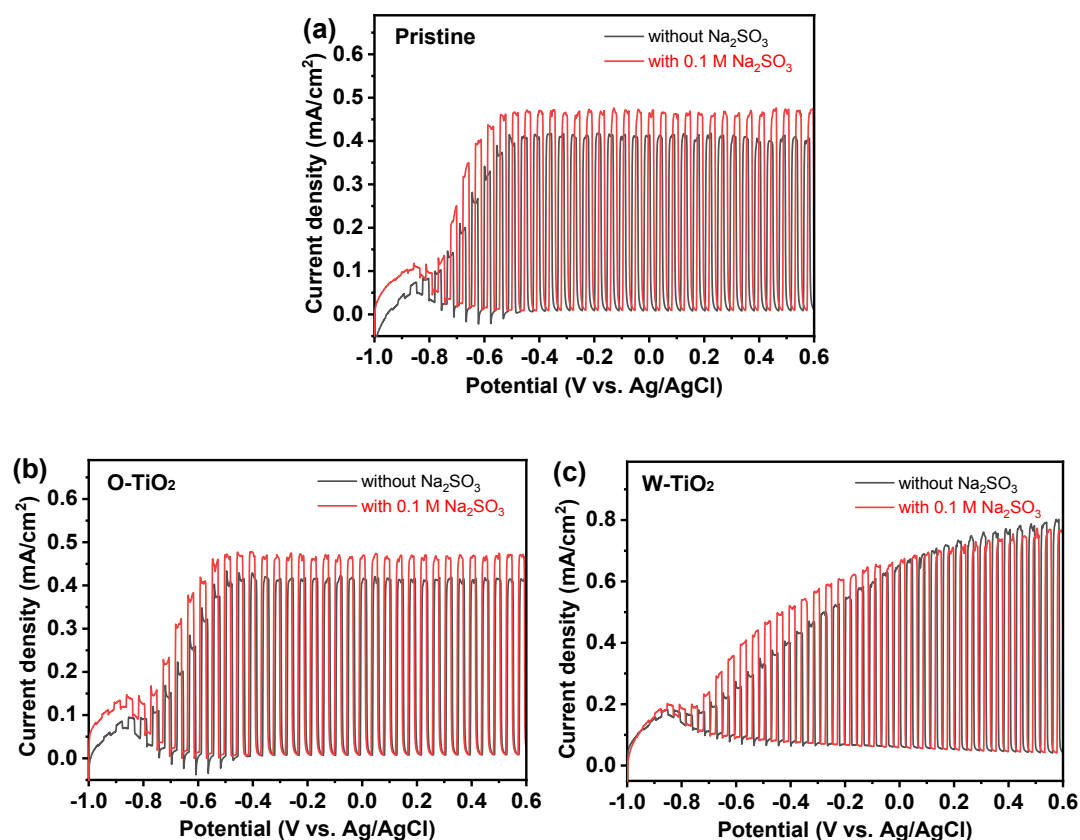


Fig. S9. Effect of sulfite ions on photocurrent density for TiO₂ nanotube electrodes (a) pristine TiO₂ nanotube photoanodes, (b) O-TiO₂ and (c) W-TiO₂ photoanodes after 10 min NaBH₄ treatment. A slight photocurrent difference was observed at the electrolyte with or without Na₂SO₃ hole scavenger, indicating that NaBH₄ treatment does not change the OER kinetics. The increasing of charge separation efficiency was the reason of the enhanced photocurrent density for W-TiO₂ photoanodes.

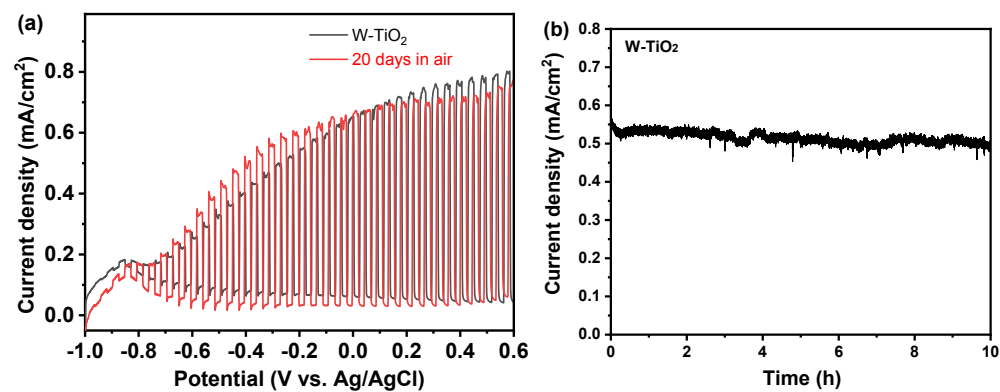


Fig. S10 (a) Photocurrent density measured in 1 M NaOH for W-TiO₂ nanotube electrodes just after 10 min NaBH₄ treatment and the same photoanodes put in air for 20 days. (b) Chronoamperometry measurement for W-TiO₂ photoanode held at 0.2 V versus Ag/AgCl in NaOH for 10 h.

References

- 1 Q. Liu, J. He, T. Yao, Z. Sun, W. Cheng, S. He, Y. Xie, Y. Peng, H. Cheng, Y. Sun, Y. Jiang, F. Hu, Z. Xie, W. Yan, Z. Pan, Z. Wu and S. Wei, *Nat. Commun.*, 2014, **5**, 5122.
- 2 H. Zhu, M. Zhao, J. Zhou, W. Li, H. Wang, Z. Xu and L. Lu, *Appl. Catal. B Environ.*, 2018, **234**, 100–108.